An asymptotic analysis of the laminar-turbulent transition of yield stress fluids in pipes

Tim G. Myers
Centre de Recerca Matemática, Barcelona, Spain
E-mail: tmyers@crm.cat

Sarah L. Mitchell
University of Limerick, Ireland
E-mail: sarah.mitchell@ul.ie

Paul Slatter
ATC Williams, Mordialloc, VIC, 3195, Australia
E-mail: pauls@atcwilliams.com.au

Abstract. The work in this paper concerns the axisymmetric pipe flow of a Herschel-Bulkley fluid, with the aim of determining a relation between the critical velocity (defining the transition between laminar and turbulent flow) and the pipe diameter in terms of the Reynolds number Re_3. The asymptotic behaviour for large and small pipes is examined and simple expressions for the leading order terms are presented. Results are then compared with experimental data. A nonlinear regression analysis shows that for the tested fluids the transition occurs at similar values to the Newtonian case, namely in the range $2100 < Re_3 < 2500$.

1. Introduction

Yield stress fluids are transported through pipes in a number of different industries and scenarios, such as the transport of crude oil, mining slurries, liquid food, concrete, bio-fluids and drilling fluids or sewage sludge, see [6, 10, 12] for example. In certain cases, many mining slurries for example, the yield stress behaviour is due to a high concentration of particles suspended in the carrier fluid. To prevent blockage of the pipe a sufficiently high velocity must be maintained, so that the flow remains turbulent, which prevents the particles from settling. However, the larger the velocity, the more expensive the operation and consequently designers and operators attempt to restrict the flow to a level only slightly above the laminar-turbulent transition point. Obviously this is a risky strategy, since errors can lead to expensive pipe blockage, and so it is critical that this transition point is accurately identified. In the following work we will focus on the flow of suspensions using the Herschel-Bulkley model. Although the Herschel-Bulkley model is not appropriate for the laminar flow of suspensions (even in the turbulent transition region most particles will settle) we will still employ it in order to derive the appropriate mathematical model. The expression for the Reynolds number in terms of the flow parameters will then be compared to experimental data to identify the laminar-turbulent transition.

The laminar-turbulent transition point for Newtonian fluids is well known and defined in terms of the Reynolds number

$$Re = \frac{\rho V D}{\eta} \ , \tag{1}$$

where ρ is the density, V the average velocity, D the pipe diameter and η the dynamic viscosity. Transition typically occurs for $Re \sim 2300$, although values between 1760 and 2300 are quoted in Kerswell [7]. This issue is discussed in great detail in the survey of Eckhardt *et al.* [3]. For yield stress fluids the matter is even less clear; one problem being that there is not a unique definition of the Reynolds number. Metzner & Reed [8] proposed a generalised Reynolds number

$$Re_{MR} = \frac{8\rho V^2}{\tau_{0_l}} \ , \tag{2}$$

where τ_{0_l} is the shear stress at the wall under laminar flow conditions. Wasp *et al.* [21] define a Reynolds number for a Bingham fluid (i.e. $n = 1$) based on the Hedström number

$$Re_W = 1500 \left(1 + \sqrt{1 + \frac{\rho D^2 \tau_y}{4500 K^2}} \right) \ , \tag{3}$$

where τ_y is the yield stress and K the consistency index. A common generalisation of the Newtonian Reynolds number, Re_w, involves defining the viscosity at the wall, so $\eta = \eta_w$ in (1), where η_w is the ratio of the shear stress and shear rate at the wall, see [2, 11, 19] for example. For a yield stress fluid flowing in a pipe, Slatter [1, 15] proposes a formulation that takes this concept even further. Instead of focussing on the flow solely at the pipe wall they include the flow in the annular region surrounding the central plug. The plug flow is neglected based on the premise that this does not form part of the sheared region, and is not behaving as a fluid. The analysis leads to what is termed Re_3

$$Re_3 = \frac{8\rho V_a^2}{\tau_y + K\left(\frac{8V_a}{D_a}\right)^n} \ , \tag{4}$$

where V_a is the average fluid velocity in the sheared annulus and D_a is the difference between the pipe diameter and the plug diameter.

Not only is the appropriate form of the Reynolds number subject to debate, there is also confusion over the value at which the transition occurs; although this is most likely fluid dependent. In [4] the flow of a Laponite fluid is investigated, using a Herschel-Bulkley model, and their experiments indicate a transition to turbulence for $Re_w \sim 3400$. Rudman *et al.* [11] suggest that as the power law exponent decreases, so the flow moves further away from Newtonian, and the transitional value of Re_w increases. Their experiments indicate that transition occurs for $Re_w \in [1300, 3000]$.

Draad *et al.* investigate polymer solutions which are modelled well by the Carreau viscosity relation (i.e. there is no yield stress). They conclude that for flow in relatively large pipes (compared to the polymer length-scale) the transition will occur around the same value as for a Newtonian solution, $Re_w \sim 2300$. This result may be related to Re_3 via the following argument. In the limit $\tau_y \to 0$ the annular velocity and diameter reduce to the average velocity and pipe diameter, $V_a \to V$, $D_a \to D$ and

$$Re_3 \to \frac{8^{1-n}\rho V^{2-n} D^n}{K} \ , \tag{5}$$

where n is the exponent in the fluid viscosity definition. The viscosity at the wall η_w is

$$\eta_w = \frac{K^{1/n}\tau_0}{(\tau_0 - \tau_y)^{1/n}} \ .$$

(Note, this may be calculated using the expression for velocity given in the following section). Combining this with the expression for V (also given in the following section) and setting $\tau_y = 0$, we determine

$$Re_w = \left(\frac{6n+2}{n}\right)^{1-n} \frac{\rho V^{2-n} D^n}{K} \ . \tag{6}$$

The expressions for Re_w and Re_3 only differ by a factor $f(n) = (8n/(6n+2))^{1-n}$. For $n \in [0.5, 1]$ the factor $f \in [0.9, 1]$ and consequently we expect that, provided $\tau_y \sim 0$ and $n \in [0.5, 1]$, the transition value for Re_3 should also be close to 2300. The experimental results of Slatter [16] confirm this by showing that a choice of Re_3 anywhere in the range $[2100, 2400]$ provides accurate results for the transition. Observe that the experimental data quoted in Table 1 in the appendix have $n > 0.59$, whereas the results of Draad *et al.* [2] have $n > 0.61$.

The principal objective of Slatter's work [12, 13, 14, 15, 16] was to establish a simple, single criterion for transition such as exists for Newtonian pipe flow, e.g. $Re = 2300$ [16]. This obviously requires an appropriate definition of the Reynolds number. In §4 we show that $Re_3 \in [2100, 2500]$ provides good agreement with experimental data and consequently is an appropriate non-dimensional parameter to categorize the behaviour of a Herschel-Bulkley fluid.

The Reynolds number depends on both the velocity and pipe diameter. To maintain turbulent flow, for a given pipe diameter, the mean fluid velocity must be kept above a critical value V_c. One focus of this work is to find a simple relation between the critical mean velocity, V_c, and the pipe diameter, D, for large pipes. For sufficiently large pipes, $D = \mathcal{O}(1)\,\mathrm{m}$, experimental observations indicate that the critical velocity becomes independent of the pipe diameter [12]. In this limit, dimensional analysis shows that the dependence of V_c then takes the form

$$V_c = C(n)\sqrt{\frac{\tau_y}{\rho}} \ . \tag{7}$$

However, the dimensional analysis cannot determine the form of the coefficient $C(n)$, which must at present be approximated numerically for a given fluid. One of our goals is therefore to find an analytical expression for $C(n)$. Our other goal is to show that Re_3 is an appropriate non-dimensional number to characterize the flow of a yield-stress fluid. Once this has been established we can then determine the correct value of Re_3 that predicts the transition to turbulence.

The structure of the paper is as follows. In §2 we quote standard results to describe the flow of a Herschel-Bulkley fluid in a pipe and consequently determine V_a and D_a which are required in the expression for Re_3 in (4). These results are then used in §3 to determine different asymptotes for the ratio of yield stress to wall shear stress: these can then be translated onto the critical velocity-pipe diameter diagram. In particular we find an analytical expression for $C(n)$. In §4 we compare our analytical model with the experimental data of Slatter [16] and use a nonlinear regression analysis to determine the best choice of Re_3.

2. Governing equations for the flow

Under conditions of fully developed, steady-state, one dimensional laminar pipe flow, a yield-stress fluid will shear in the annular region next to the pipe wall. Near the centre of the pipe, where the applied shear stresses are less than the yield stress, there will be a solid, unsheared plug which is carried along by the applied pressure gradient at the maximum fluid velocity: this

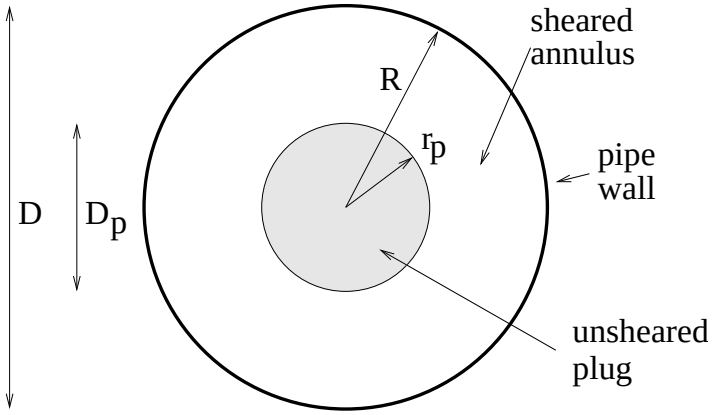

Figure 1. *Steady, unidirectional flow geometry.*

is depicted in Figure 1. The velocity is given by $\mathbf{u} = (0, w(r))$, where w is the velocity along the axis.

Velocity and shear stress relations for axisymmetric pipe flow are well known. For unidirectional flow, the shear stress in the annular region for a Herschel-Bulkley fluid is defined by

$$\tau = -\tau_y - K\left(-\frac{\partial w}{\partial r}\right)^n \ , \qquad |\tau| > \tau_y \ , \tag{8}$$

where K is the consistency index and τ_y the yield stress. In the plug region $0 \le r \le r_p$, where $|\tau| < \tau_y$, the velocity is constant $w_r = 0$. In the annular region $r_p \le r \le R$ the velocity profile is

$$w = \frac{2n}{(n+1)p_z K^{1/n}}\left[\left(-\frac{p_z r}{2} - \tau_y\right)^{(n+1)/n} - \left(-\frac{p_z R}{2} - \tau_y\right)^{(n+1)/n}\right] \ , \tag{9}$$

where p_z is the pressure gradient. Since $\tau = -\tau_y$ at $r = r_p$ the plug radius can be expressed as

$$r_p = -\frac{2\tau_y}{p_z} \ . \tag{10}$$

Substituting for $r = r_p$ in (9) determines the plug velocity

$$w_p = -\frac{2n}{(n+1)p_z K^{1/n}}\left(-\frac{p_z R}{2} - \tau_y\right)^{(n+1)/n} \ . \tag{11}$$

Equation (4) for Re_3 requires expressions for the annular velocity V_a and the diameter of the annular region D_a. The latter quantity is simply

$$D_a = 2(R - r_p) \ , \tag{12}$$

where r_p is defined by equation (10). The annular velocity $V_a = Q_a/A_a$ requires an expression for the annular flux which is the difference between the total flux and the flux of the plug region

$$Q_a = Q - Q_p = Q - w_p \pi r_p^2 \ , \tag{13}$$

and so

$$V_a = \frac{Q - w_p \pi r_p^2}{\pi (R^2 - r_p^2)} \ . \tag{14}$$

The total flux is $Q = VA = V\pi R^2$ where V is the mean velocity in the pipe:

$$V = \frac{2\pi}{\pi R^2}\left[\int_0^{r_p} r w_p \, \mathrm{d}r + \int_{r_p}^{R} r w \, \mathrm{d}r\right] \tag{15}$$

$$= \frac{Dn}{2K^{1/n}\tau_0^3}(\tau_0 - \tau_y)^{(n+1)/n}\left[\frac{(\tau_0 - \tau_y)^2}{3n+1} + \frac{2\tau_y(\tau_0 - \tau_y)}{2n+1} + \frac{\tau_y^2}{n+1}\right] . \tag{16}$$

From the definition of the stress we find the ratio $r_p/R = \tau_y/\tau_0$. Using this and the definitions of V and w_p we may write V_a in (14) as

$$V_a = \frac{V\pi R^2 - w_p \pi r_p^2}{\pi (R^2 - r_p^2)} = \frac{V\tau_0^2 - w_p \tau_y^2}{\tau_0^2 - \tau_y^2} = \frac{Dn}{2K^{1/n}} \frac{(\tau_0 - \tau_y)^{(n+1)/n}}{\tau_0(\tau_0 + \tau_y)}\left[\frac{\tau_0 - \tau_y}{3n+1} + \frac{2\tau_y}{2n+1}\right] . \tag{17}$$

Similarly D_a from (12) becomes

$$D_a = \frac{D(\tau_0 - \tau_y)}{\tau_0} \ . \tag{18}$$

Substitution of the above expressions for V_a and D_a, equations (17, 18), into the definition of Re_3 (4) therefore gives

$$Re_3 = \frac{\rho D^2}{8K^{2/n}} \frac{(\tau_0 - \tau_y)^{2(n+1)/n}\tau_0^{-2}(\tau_0 + \tau_y)^{-2}[a(\tau_0 - \tau_y) + 2b\tau_y]^2}{\tau_y + (\tau_0 - \tau_y)(\tau_0 + \tau_y)^{-n}[a(\tau_0 - \tau_y) + 2b\tau_y]^n} \ , \tag{19}$$

while the expression for V in (16) becomes

$$V = \frac{D}{8K^{1/n}}(\tau_0 - \tau_y)^{(n+1)/n}\tau_0^{-3}\left[a(\tau_0 - \tau_y)^2 + 2b\tau_y(\tau_0 - \tau_y) + c\tau_y^2\right] , \tag{20}$$

where, to simplify notation, we set

$$a = \frac{4n}{3n+1} \ , \qquad b = \frac{4n}{2n+1} \ , \qquad c = \frac{4n}{n+1} \ . \tag{21}$$

3. Asymptotic analysis

Now that Re_3 and the average velocity (19, 20) have been calculated we can determine the relation between the Reynolds number, the mean velocity V and the pipe diameter D. The aim of this work is to find the critical velocity, $V = V_c$, above which the flow is turbulent. This should occur at a specific value of Re_3. The following analysis leads to a relation of the form $V = f(Re_3, D)$ and by choosing a specific value of Re_3 we determine the relation between V_c and D. We can then show, from a nonlinear regression analysis using experimental data [12, 16], that the transition to turbulent flow occurs in the range $2100 < Re_3 < 2500$.

We find it convenient to introduce the parameter $\mathcal{A} = \tau_0/\tau_y = R/r_p$, which is the ratio of wall shear stress to yield stress or equivalently the pipe radius to the plug radius. In the following we will assume that the fluid properties are fixed and so control $\mathcal{A}$ by varying the pipe diameter. In the small D limit the high shear rates required to move the fluid will confine the

plug to a small region near $r = 0$. This means that $A = R/r_p \gg 1$ as $D \to 0$. Experimental results, see [12] for example, show that for large D the critical velocity approaches a constant value. This is confirmed by dimensional analysis in [12] for the case $n < 1$. For the large D limit, letting $D \to \infty$ in equation (20) shows that to prevent $V \to \infty$ then $\tau_0 \to \tau_y$ (in fact $\tau_o - \tau_y \propto D^{-n/(n+1)}$) and hence $\mathcal{A} \to 1^+$.

In the following analysis it is convenient to set $\tau_0 = \mathcal{A}\tau_y$, for $\mathcal{A} > 1$, and then the large D limit corresponds to $\mathcal{A} \approx 1$, whereas the small D limit corresponds to $\mathcal{A} \gg 1$. Substitution of $\tau_0 = \mathcal{A}\tau_y$ into (19) and (20) gives

$$Re_3 = \frac{\rho D^2 \tau_y^{2/n-1}}{8K^{2/n}} \frac{(\mathcal{A}-1)^{2(n+1)/n}\mathcal{A}^{-2}(\mathcal{A}+1)^{-2}[a(\mathcal{A}-1)+2b]^2}{1+(\mathcal{A}-1)(\mathcal{A}+1)^{-n}[a(\mathcal{A}-1)+2b]^n} , \tag{22}$$

$$V = \frac{D\tau_y^{1/n}}{8K^{1/n}}(\mathcal{A}-1)^{(n+1)/n}\mathcal{A}^{-3}\Big[a(\mathcal{A}-1)^2+2b(\mathcal{A}-1)+c\Big] . \tag{23}$$

We now consider the cases $\mathcal{A} \approx 1$ and $\mathcal{A} \gg 1$ separately.

3.1. The $\mathcal{A} \approx 1$ (large D) asymptote

Since $\mathcal{A} \approx 1$ (but strictly $\mathcal{A} > 1$ to allow some flow) we write $\mathcal{A}$ as the following expansion:

$$\mathcal{A} - 1 = \alpha_0\epsilon + \alpha_1\epsilon^2 + \alpha_2\epsilon^3 + ... , \tag{24}$$

where $\alpha_i = \mathcal{O}(1)$, $\alpha_0 > 0$ and $0 < \epsilon \ll 1$. Substitution of (24) into (22) leads to

$$\begin{aligned} Re_3 = \frac{\rho D^2 \tau_y^{2/n-1}}{8K^{2/n}} b^2(\alpha_0\epsilon)^{2(n+1)/n}\Bigg[1 &+ \left\{\frac{a}{b} - 3 - b^n + \frac{2(n+1)}{n}\frac{\alpha_1}{\alpha_0^2}\right\}\alpha_0\epsilon \\ &+ \left\{\frac{a^2}{4b^2} + \frac{23}{4} - \frac{3a}{b} + \frac{nb^n}{2}\left(1-\frac{a}{b}\right) - \left(\frac{3n+2}{n}\left(3-\frac{a}{b}\right)+b^n\right)\frac{\alpha_1}{\alpha_0^2}\right. \\ &\left. + \frac{(n+1)(n+2)}{n^2}\frac{\alpha_1^2}{\alpha_0^4} + \frac{2(n+1)}{n}\frac{\alpha_2}{\alpha_0^3}\right\}(\alpha_0\epsilon)^2 + ...\Bigg] , \end{aligned} \tag{25}$$

and in (23) we now have

$$\begin{aligned} V = \frac{D\tau_y^{1/n}}{8K^{1/n}} c(\alpha_0\epsilon)^{(n+1)/n}\Bigg[1 &+ \left(\frac{2b}{c} - 3 + \frac{n+1}{n}\frac{\alpha_1}{\alpha_0^2}\right)\alpha_0\epsilon \\ &+ \left\{6 + \frac{a}{c} - \frac{6b}{c} + \frac{2n+1}{n}\left(\frac{2b}{c}-3\right)\frac{\alpha_1}{\alpha_0^2} + \frac{n+1}{2n^2}\frac{\alpha_1^2}{\alpha_0^4} + \frac{n+1}{n}\frac{\alpha_2}{\alpha_0^3}\right\}(\alpha_0\epsilon)^2 + ...\Bigg] . \end{aligned} \tag{26}$$

The expression for $\alpha_0\epsilon$ is found from the leading order term in (25) and so

$$\alpha_0\epsilon = \left(\frac{8Re_3K^{2/n}}{\rho\tau_y^{(2-n)/n}}\right)^{n/2(n+1)}(bD)^{-n/(n+1)} . \tag{27}$$

Setting the higher order correction terms to zero determines α_1, α_2. Substitution of $\alpha_0, \alpha_1, \alpha_2$ into (26) gives V as a function of D.

If we simply consider the leading order term and substitute for $\alpha_0\epsilon$, via (27), into (26) then V becomes

$$V \sim \frac{c}{b}\sqrt{\frac{Re_3\tau_y}{8\rho}} = C(n)\sqrt{\frac{\tau_y}{\rho}} , \qquad C(n) = \frac{2n+1}{n+1}\sqrt{\frac{Re_3}{8}} . \tag{28}$$

As discussed in the introduction, finding the expression in (28) was one of the main goals of the original analysis [9]. This equation identifies the asymptote as $D \to \infty$ and the form of the fluid constant $C(n)$. However, including the correction terms $\mathcal{O}[\epsilon]$ and $\mathcal{O}[\epsilon^2]$ in (26) means that we can find the form of the curve for smaller D and so get closer to the transition between the small and large D asymptotes. This can be seen in more detail in the Results section below. Note that the condition $\alpha_0\epsilon \ll 1$ provides a limit for the pipe diameter

$$D \gg \frac{1}{b}\left(\frac{8Re_3K^{2/n}}{\rho\tau_y^{(2-n)/n}}\right)^{1/2} . \tag{29}$$

The large D expansion can also be derived by considering the expressions for Re_3 and V in (19) and (20) directly. Since $\tau_0 \to \tau_y$ in this limit, a high proportion of the slurry will be at the yield stress and consequently the plug occupies most of the pipe. Experiments also show that the transition velocity V_c becomes independent of D as $D \to \infty$ [12]. From examining (20) it is clear that this can only occur if $(\tau_0 - \tau_y)^{(n+1)/n} = \mathcal{O}[D^{-1}]$. We could therefore look for an expansion of $\tau_0 - \tau_y$ in terms of the small parameter $\epsilon = D^{-n/(n+1)}$, namely

$$\tau_0 - \tau_y = \alpha_0 D^{-n/(n+1)} + \alpha_1 D^{-2n/(n+1)} + \mathcal{O}((D^{-n/(n+1)})^3) = \alpha_0\epsilon + \alpha_1\epsilon^2 + \mathcal{O}(\epsilon^3) .$$

This method yields the same expansions for Re_3 and V and is discussed in more detail in [9].

3.2. The large $\mathcal{A}$ (small D) asymptote

In this case $\mathcal{A} \gg 1$ and so we consider an expansion in terms of the small parameter $\mathcal{B} = 1/\mathcal{A}$. Rewriting Re_3 and V from (22) and (23) in terms of $\mathcal{B}$ gives

$$Re_3 = \frac{\rho D^2\tau_y^{2/n-1}}{8K^{2/n}} \frac{(1-\mathcal{B})^{2(n+1)/n}\mathcal{B}^{1-2/n}(1+\mathcal{B})^{-2}[a(1-\mathcal{B})+2b\mathcal{B}]^2}{\mathcal{B}+(1-\mathcal{B})(1+\mathcal{B})^{-n}[a(1-\mathcal{B})+2b\mathcal{B}]^n} , \tag{30}$$

$$V = \frac{D\tau_y^{1/n}}{8K^{1/n}}\mathcal{B}^{-1/n}(1-\mathcal{B})^{(n+1)/n}\Big[a(1-\mathcal{B})^2 + 2b\mathcal{B}(1-\mathcal{B}) + c\mathcal{B}^2\Big] . \tag{31}$$

Suppose $\mathcal{B}$ is expanded as

$$\mathcal{B} = \beta_0\epsilon + \beta_1\epsilon^2 + \beta_2\epsilon^3 + ... , \tag{32}$$

where $\beta_i = \mathcal{O}(1)$, $\beta_0 > 0$ and $0 < \epsilon \ll 1$. Substitution into (30) and (31) leads to expansions

$$\begin{aligned} Re_3 = \frac{\rho D^2\tau_y^{2/n-1}}{8K^{2/n}}a^{2-n}(\beta_0\epsilon)^{1-2/n}\Bigg[1 &+ \left\{\frac{2b(2-n)}{a} - \frac{5n+2-2n^2}{n} - a^{-n} + \frac{n-2}{n}\frac{\beta_1}{\beta_0^2}\right\}\beta_0\epsilon \\ &\left\{\frac{n-n^2+2}{2}\left(-1+\frac{2b}{a}\right)^2 + \frac{n^3+n^2-8n-4}{n}\left(-1+\frac{2b}{a}\right)\right. \\ &+\left(\frac{2b(4n-n^2-4}{an} + \frac{2n^3-11n^2+8n+4}{n^2} - a^{-n}\right)\frac{\beta_1}{\beta_0^2} \\ &\left.-\frac{3n^3+n^4-16n^2-14n-4}{2n^2} - \frac{n-2}{n^2}\frac{\beta_1^2}{\beta_0^4} + \frac{n-2}{n}\frac{\beta_1}{\beta_0^2}\right\}(\beta_0\epsilon)^2 + ...\Bigg] , \end{aligned} \tag{33}$$

and

$$V = \frac{D\tau_y^{1/n}}{8K^{1/n}}a(\beta_0\epsilon)^{-1/n}\left[1 + \left(\frac{2b}{a} - 2 - \frac{n+1}{n} - \frac{1}{n}\frac{\beta_1}{\beta_0^2}\right)\beta_0\epsilon\right.$$

$$+\left\{1+\frac{c}{a}-\frac{2b}{a}+\frac{n-1}{2n^2}-\frac{2(n+1)}{n}\left(-1+\frac{b}{a}\right)\right.$$
$$\left.+\left(\frac{2b}{a}-2+\frac{1-n^2}{n}-\frac{2}{n}\left(-1+\frac{b}{a}\right)\right)\frac{\beta_1}{\beta_0^2}+\frac{n+1}{2n^2}\frac{\beta_1^2}{\beta_0^4}-\frac{1}{n}\frac{\beta_2}{\beta_0^3}\right\}(\beta_0\epsilon)^2+...\Bigg] \ . \quad (34)$$

From the leading order term in (33) we obtain an expression for $\beta_0\epsilon$

$$\beta_0\epsilon=\tau_y\left(\frac{8Re_3K^{2/n}}{\rho}\right)^{n/(n-2)}a^nD^{2n/(2-n)} \ , \quad (35)$$

with expressions for $\beta_1\epsilon^2$ and $\beta_2\epsilon^3$ found by setting the $\mathcal{O}[\epsilon]$ and $\mathcal{O}[\epsilon^2]$ terms to zero. Substituting $\beta_0\epsilon$ into the dominant term in (34) gives

$$V\sim\left(\frac{8^{n-1}KRe_3}{\rho D^n}\right)^{1/(2-n)} \ , \quad (36)$$

as the leading order term for the velocity in the small D limit. Note that $V\sim D^{-n/(2-n)}$ and so in the Bingham limit $n=1$, this implies that $V\sim 1/D$ as $D\to 0$. So, for small D the critical velocity (to leading order) is independent of the yield stress τ_y.

The condition $\beta_0\epsilon\ll 1$ indicates that the analysis is valid for

$$D\ll a^{-1+n/2}\left(\frac{8Re_3K^{2/n}}{\rho\tau_y^{(2-n)/n}}\right)^{1/2} \ . \quad (37)$$

As discussed in [9], an alternative way to derive (36) is to note that, since $r_p\ll R$ in the limit $D\to 0$, then $D_a\approx D$ and $V_a\approx V=\frac{D\tau_0^{1/n}a}{8K^{1/n}}$ to leading order in τ_y/τ_0. Then Re_3 in (4) becomes

$$Re_3\approx\frac{8\rho V^2}{K}\left(\frac{D}{8V}\right)^n \ , \quad (38)$$

where the τ_y term in the denominator has been neglected since $\tau_y\ll K\left(\frac{8V_a}{D_a}\right)^n$ for $\tau_0\gg\tau_y$. Rearranging (38) then gives (36) directly. Although this might seem like a more direct way to find an expression for the velocity, the analysis in terms of parameters $\mathcal{A}$ and $\mathcal{B}$ allows us to obtain the higher order corrections in a systematic way.

We now compare the large and small D asymptotic solutions with the exact solution and experimental data.

4. Results

The results are taken from a series of experiments described in [12, 16]: a number of fluids were pumped through a pipe test rig, over a range of flow rates, and the average velocity measured for a prescribed pressure gradient. The data points and fluid properties are provided in Table 1. Note that some obvious outliers in the data sets were omitted from our calculations. In laminar flow, the measured velocity agrees closely with that predicted by equation (16). When the flow becomes turbulent there is a marked departure between the measured and predicted values. This behaviour is depicted (in an idealised fashion) in Figure 2. The data points for V_c shown in Table 1 were extracted from pipe flow curves of the form shown in the figure using a normalised adherence function, see [17]. Note, transition phenomena, such as puffs, streaks etc.,

Data Set	ρ	τ_y	K	n	Data values (D_i, V_{ci})
A	1061.264	1.04	0.0136	0.8031	$(0.005623, 1.458)$, $(0.013214, 1.0725)$, $(0.0216, 0.945)$
B	1071.234	1.88	0.0102	0.8428	$(0.005623, 1.4)$, $(0.013214, 1.32)$, $(0.0216, 1.134)$, $(0.140512, 1.05)$, $(0.207, 1.035)$
C	1099.2	5.8	0.0176	0.8154	$(0.079, 1.95)$, $(0.140512, 1.875)$, $(0.207, 1.87)$
D	1105.034	4.18	0.0351	0.719	$(0.005623, 2.11)$, $(0.013214, 1.98)$, $(0.0216, 1.62)$, $(0.140512, 1.5152)$, $(0.207, 1.55)$
E	1176	3.91	0.0105	0.972	$(0.0216, 1.935)$, $(0.140512, 1.655)$, $(0.207, 1.61)$
F	1320.1	5.48	0.1239	0.6363	$(0.0216, 1.79)$, $(0.079, 1.74)$, $(0.207, 1.553)$
G	1394.35	8.02	0.135	0.5911	$(0.079, 1.93)$, $(0.140512, 1.94)$, $(0.207, 1.87)$
H	1501.276	8.0	0.03708	0.87907	$(0.01337, 3.29)$, $(0.02838, 2.33)$, $(0.0042, 5.68)$

Table 1. *Experimental data values [12, 16].*

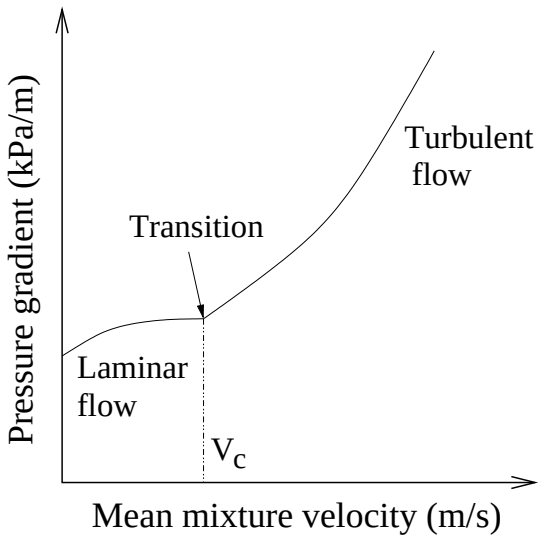

Figure 2. *Schematic of velocity against pressure gradient for water and slurry flows.*

are observed at values below V_c but these do not cause the pipe flow data to deviate from the laminar curve.

In the previous section we determined expressions for V_c in both the large and small D limits. To enable a comparison with the exact relation (20), with τ_0 found by solving the nonlinear expression in (19), we must obtain a value for Re_3 which gives the best fit to the experimental data. Equations (19) and (20) provide a relation between V (or V_c), Re_3 and D, where we must eliminate the unknown τ_0. One goal of this work is to determine the value for Re_3 that best predicts the transition. We calculate this using a nonlinear regression package provided on StatsPages.net [20]. For each given data point (D_i, V_i) we can determine a value for τ_{0i} using

(20). Then, re-writing (19) as

$$y = \frac{\tau_y + (\tau_0 - \tau_y)(\tau_0 + \tau_y)^{-n}[a(\tau_0 - \tau_y) + 2b\tau_y]^n}{(\tau_0 - \tau_y)^{2(n+1)/n}\tau_0^{-2}(\tau_0 + \tau_y)^{-2}[a(\tau_0 - \tau_y) + 2b\tau_y]^2} = \frac{\rho D^2}{8K^{2/n}Re_3} ,$$

we can determine a value for the unknown parameter Re_3 using the points (D_i, y_i). These values and the restrictions on D for the small and large diameter limits are given in Table 2 for each data set.

Data Set	Re_3	Limits (29), (37)
A	2135.5 ± 12.4	$D \gg 0.015$, $D \ll 0.019$
B	2148.5 ± 3.8	$D \gg 0.009$, $D \ll 0.012$
C	2402.7 ± 10.6	$D \gg 0.007$, $D \ll 0.008$
D	2330.0 ± 21.2	$D \gg 0.009$, $D \ll 0.012$
E	2554.6 ± 8.8	$D \gg 0.014$, $D \ll 0.019$
F	2109.6 ± 23.4	$D \gg 0.019$, $D \ll 0.024$
G	2361.9 ± 30.7	$D \gg 0.010$, $D \ll 0.012$
H	2374.0 ± 66.5	$D \gg 0.017$, $D \ll 0.023$

Table 2. *Best fit values of Re_3 for each data set.*

In Figures 3 and 4 we show plots of V_c against D for eight different Herschel-Bulkley fluids. The data points are denoted by a '*'. The solid line is the exact solution obtained by numerically solving equations (19) and (20). On the right hand side of each figure there are also three sets of curves. The lowest, represented by a dotted line, is the leading order solution for large D. It is clear from these plots that the critical velocity is independent of the pipe diameter in this limit. The solutions to first and second order are shown as dot-dash and dashed lines respectively. Similarly, on the left hand side are the three small D solutions. Finally, the two vertical lines represent the limit of validity for each expansion, which is given in the final column of Table 2. Note that these limits in fact overlap, in the sense that the small D limit is the right hand line and the large D limit is the left hand line. However, the criteria is that D is either much greater or much less than these limits and it is clear that, in most cases, the leading and first order solutions break down well before reaching these lines. Each figure requires a value for the critical Re_3, obtained by the nonlinear regression, these values are given in Table 2. Since the figures all take the same format we will only discuss the first, Figure 3 for Data Set A, in detail. In this case, the nonlinear regression, using 3 data points, indicates $Re_3 = 2135.5 \pm 12.4$. This small error is reflected in the fact that the exact solution, using $Re_3 = 2135.5$, appears to pass through all the data points. The leading order solution for large D provides an excellent approximation for pipe diameters around 1m (of the order 0.3%). Below this value the leading order solution predicts values less than the exact solution, with the accuracy decreasing with pipe diameter. The second order approximation appears accurate down to around 2cm (with an error around 5%). The restriction on D, given by equation (29), indicates that we require $D \gg 1.5$cm. For Data Set B we have more data points and find $Re_3 = 2148.5 \pm 3.8$. The two data points for large D sit on the exact solution curve, which at this stage is indistinguishable from the first and second order asymptotic expansions. The data point for the smallest value of D is somewhat below the exact solution curve. Although we do not have a great amount of data for small diameter pipes, it is clear from Data Set H, shown in Figure 4, that the exact solution does not in general over-predict V_c for small D.

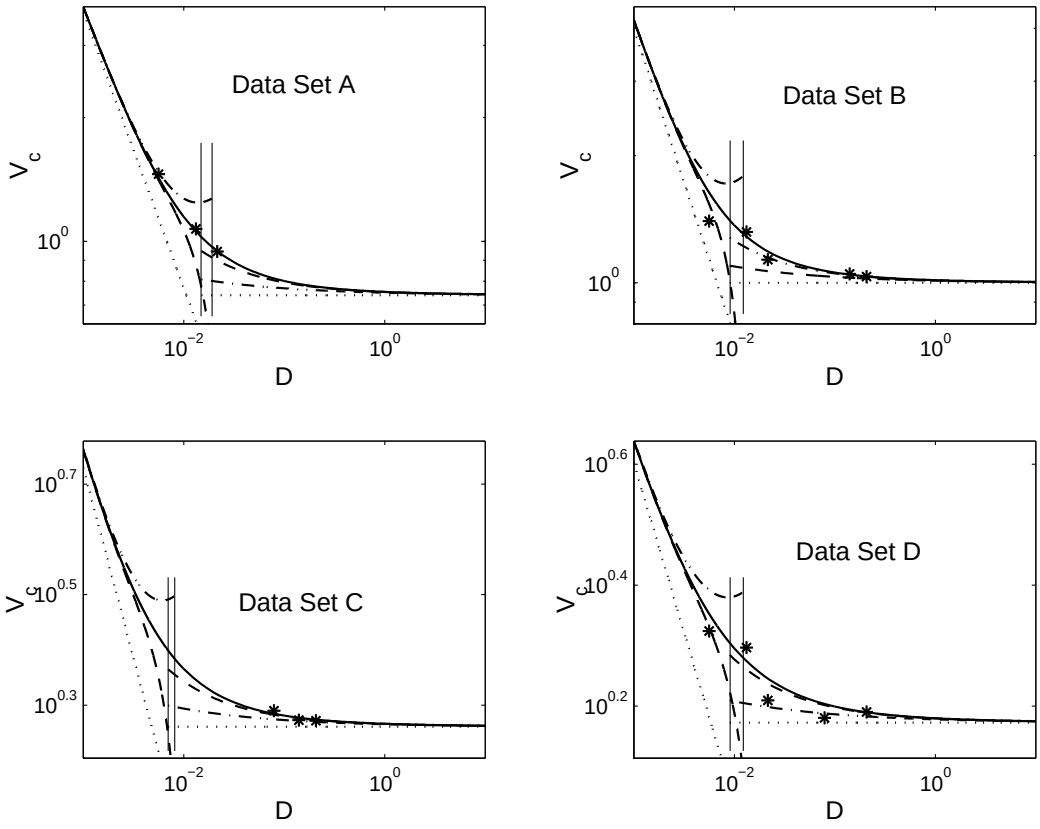

Figure 3. *Plot of critical velocity against pipe diameter for Data Sets A-D. The solid line denotes the exact solution, the dotted, dot-dashed and dashed lines denote the small (left) and large (right) D asymptotes for leading, first and second order corrections respectively.*

5. Conclusion and discussion

The primary aims of this paper were:
a) to determine whether Re_3 is a suitable expression for the non-dimensional Reynolds number which characterizes the flow of a yield-stress fluid and, if so, to find the best choice of Re_3 that predicts the transition to turbulence;
b) to investigate the asymptotic relation between the critical velocity and pipe diameter and, in particular, to determine the unknown coefficient $C(n)$ identified by dimensional analysis.

In general it appears that the form of Re_3 described by equations (19) and (20) leads to excellent agreement with the data for both large and small diameter pipes, and consequently it seems to be an appropriate non-dimensional grouping to characterize the flow. The nonlinear regression indicates that the transition to turbulence occurs for values of Re_3 within the range 2100 – 2500. This is in keeping with quoted values for a Newtonian fluid. There appears to be no obvious connection between the fluid properties and the predicted value of Re_3. For example, the three data sets that show $Re_3 \sim 2100$ have yield stresses ranging from 1.04 to 5.48 $\mathrm{N/m^2}$ and a power n between 0.84 and 0.64. The highest value of Re_3 predicted, $Re_3 \sim 2550$, occurred with the fluid most close to the Newtonian power, $n = 0.97$.

For fluids with an exponent $n \approx 1$, it is perhaps not surprising that the transition predicted by Re_3 is similar to Newtonian predictions. The thinking behind Re_3 is that only flowing material should be considered; the unyielded material is not included in the calculation. This is accounted for by the shift, of magnitude τ_y, in the denominator of Re_3. So, when $n = 1$,

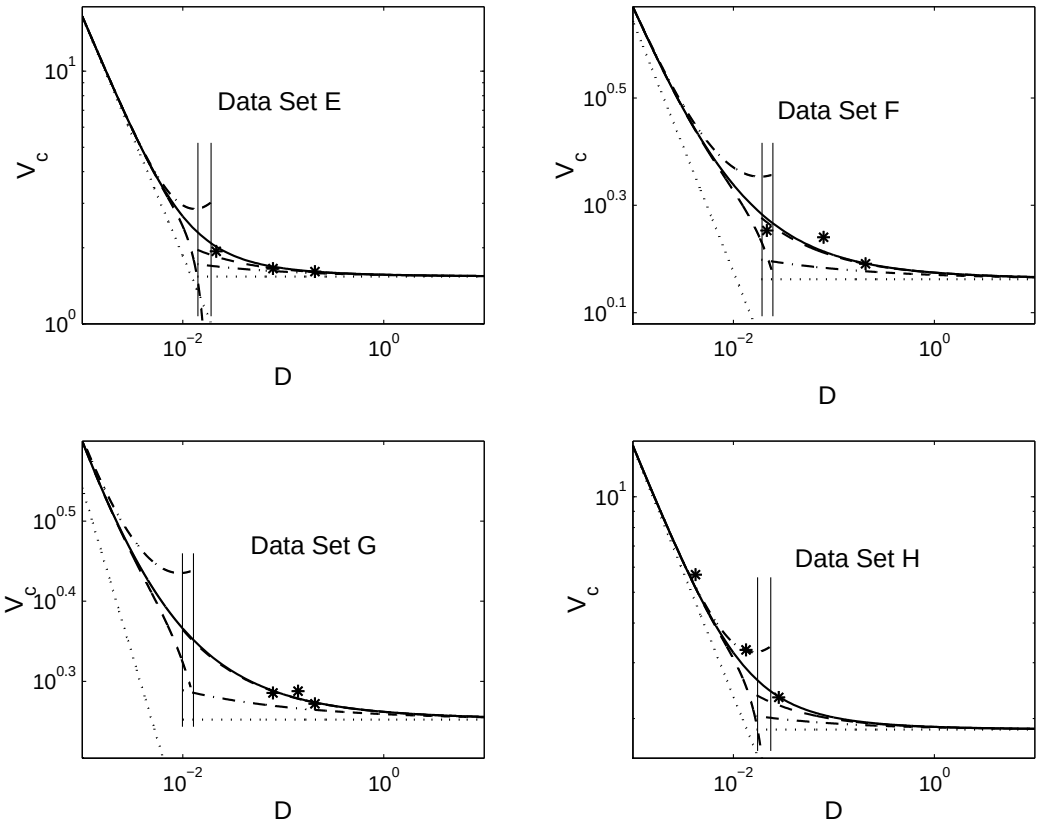

Figure 4. *Plot of critical velocity against pipe diameter for Data Sets E-H. The solid line denotes the exact solution, the dotted, dot-dashed and dashed lines denote the small (left) and large (right) D asymptotes for leading, first and second order corrections respectively.*

the flowing material exhibits Newtonian behaviour, the unyielded fluid is neglected and Re_3 is equivalent to the Newtonian Reynolds number (where V is replaced by V_a and D by D_a). Other definitions of the Reynolds number for a yield stress fluid take into account the unyielded material and so should not necessarily be expected to equate to the Newtonian value. For $n \neq 1$ the results of Draad *et al.* [2] suggest that with no yield stress the transition occurs for values of Re_w similar to the Newtonian case. Since $Re_3 \approx Re_w$ when $\tau_y = 0$ and $n \in [0.5, 1]$, by the same argument we should again expect transition to occur for $Re_3 \sim 2300$ when $\tau_y \neq 0$. Note, our experimental results satisfy the criteria since $n > 0.59$ for all cases; Draad *et al.* [2] have $n > 0.61$.

The actual calculation of Re_3 for given flow conditions is not as straightforward as for the Newtonian problem. It requires the calculation of the average annular velocity and the annular diameter which in turn require the average velocity and the wall stress. To determine a relation between V_c and D the wall stress must then be eliminated from expressions for Re_3 and V, given by equations (19) and (20). Clearly it is desirable to have a simple relation between the critical velocity and the pipe diameter, particularly for relatively large pipes which are of interest to a number of industries. Previously, dimensional analysis had shown that in the large pipe limit $V_c = C(n)\sqrt{\tau_y/\rho}$, where the coefficient $C(n)$ had to be calculated experimentally or numerically for a given fluid. The leading order term of the asymptotic analysis led to a simple form for $C(n)$, in terms of n and Re_3, and also indicated the lower limit for the pipe diameter when this

could be applied. The first and second order corrections permitted this approximation to be extended to lower values of D. An asymptotic expansion for small diameter pipes showed that at leading order $V_c \propto D^{n/(n-2)}$.

Our work provides evidence confirming two physical facts of profound practical and theoretical importance for viscoplastic fluids:

- Firstly, at small pipe diameter, the critical velocity V_c is independent of the yield stress;
- Secondly, at large pipe diameter, V_c is independent of the pipe diameter and the consistency index, and the yield stress plays a dominant role.

Asymptotic relations describing both these conditions have been provided and tested against experimental data.

There is obvious scope for extending this work, to match the large and small diameter expansions to give a complete expression for V_c against D. We did not carry this out for two reasons. Firstly, our interest lays primarily with the large pipe limit, which is applicable to the transport of mining waste for example. Secondly, in our examples, the transition region was relatively small, typically between 1mm and 1cm, and the work involved seemed greater than simply calculating the exact solution numerically.

Acknowledgments
Financial support was provided through a Ministerio de Ciencia e Innovación grant MTM2014-56218 and the Mathematics Applications Consortium for Science and Industry (www.macsi.ul.ie) based at the University of Limerick, funded by the Science Foundation Ireland grant 12/IA/1683.

References

[1] R.P. Chhabra and J.F. Richardson, Non-Newtonian flow in the process industries, Butterworth-Heinemann, 1999.
[2] A.A. Draad and G.D.C. Kuiken and F.T.M. Nieuwstadt, Laminar-turbulent transition in pipe flow for Newtonian and non-Newtonian fluids, J. Fluid Mech., 1998, 377, 267-312.
[3] B. Eckhardt and T.M. Schneider, and B. Hof and J. Westerweel., Turbulence transition in pipe flow, Ann. Rev. Fluid Mech., 2007, 39, 447-468.
[4] M.P. Escudier and F. Presti, Pipe flow of a thixotropic liquid, J. Non-Newtonian Fluid Mech., 1996, 62, 291-306.
[5] G.W. Govier and K. Aziz, The Flow of Complex Mixtures in Pipes, Litton Educational Pub. Inc., 1972.
[6] H.C. Honey and W.A. Pretorius, Laminar flow pipe hydraulics of pseudoplastic-thixotropic sewage sludges, Water SA, 2000, 26(1), 19-25.
[7] R.R. Kerswell, Recent progress in understanding the transition to turbulence in a pipe, Nonlinearity, 2005, 18, 17-44.
[8] A.B. Metzner and J.C. Reed, Flow of non-Newtonian fluids - correlation of the laminar, transition and turbulent flow regions, AIChE J., 1955, 1(4).
[9] S.L. Mitchell & T.G. Myers, The laminar-turbulent transition of yield stress fluids in large pipes, Mathematics in Industry Study Group, 2007, January, University of Witwatersrand.
[10] J. Peixinho and C. Nouar and C. Desaubry and B.Théron, Laminar transitional and turbulent flow of yield stress fluid in a pipe, J. Non-Newtonian Fluid Mech., 2005, 128, 172-184.
[11] M. Rudman and H.M. Blackburn and L.J.W. Graham and L. Pullum, J. Non-Newtonian Fluid Mech., 2004, 118, 33-48.
[12] P.T. Slatter, The role of the yield stress on the laminar/turbulent transition, Ninth Int. Conf. on Transport & Sedimentation of Solid Particles, 1997, 547-561, Cracow, ISBN 8385582232.
[13] P.T. Slatter and E.J. Wasp, The laminar/turbulent transition in large pipes, Ninth Int. Conf. on Transport & Sedimentation of Solid Particles, 2001, 389-399, Wroclaw, September, ISBN 83-87866-12-1.
[14] P.T. Slatter and J.H. Lazarus, Critical flow in slurry pipelines, 12th Int. Conf. on slurry handling and pipeline transport, Hydrotransport 12, 1993, 639.
[15] P.T. Slatter, The role of rheology in the pipelining of mineral slurries, Min. Pro. Ext. Met. Rev., 1999, 20, 281-300.

[16] P.T. Slatter, The laminar/turbulent transition prediction for non-Newtonian slurries, Proc. Int. Conf. Problems in Fluid Mechanics and Hydrology", Academy of Sciences of the Czech Republic, 2001, Prague, June, 247-256, ISBN 80 238 3824 5.
[17] P.T. Slatter, A new friction factor for yield stress fluids, British Hydrodynamic Research Group, 14th Int. Conf. on slurry handling and pipeline transport, Hydrotransport 14, 1999, Maastricht, Sept., 255 - 265, ISBN 186058 213 3.
[18] R.J. Soto and V.L. Shah, Entrance flow of a yield-power law fluid, Appl. Sci. Res., 1976, 32, 73-85.
[19] F.T. Pinho and J.H. Whitelaw, Flow of non-Newtonian fluids in a pipe, J. Non-Newtonian Fluid Mech., 1990, 34, 129-144.
[20] StatsPages.net http://statspages.org/nonlin.html, last accessed Sept 23rd 2016.
[21] E.J. Wasp and J.P. Kenny and R.L. Gandhi, Solid-liquid flow: slurry pipeline transportation, Trans Tech Publications, 1977, New York.